S1

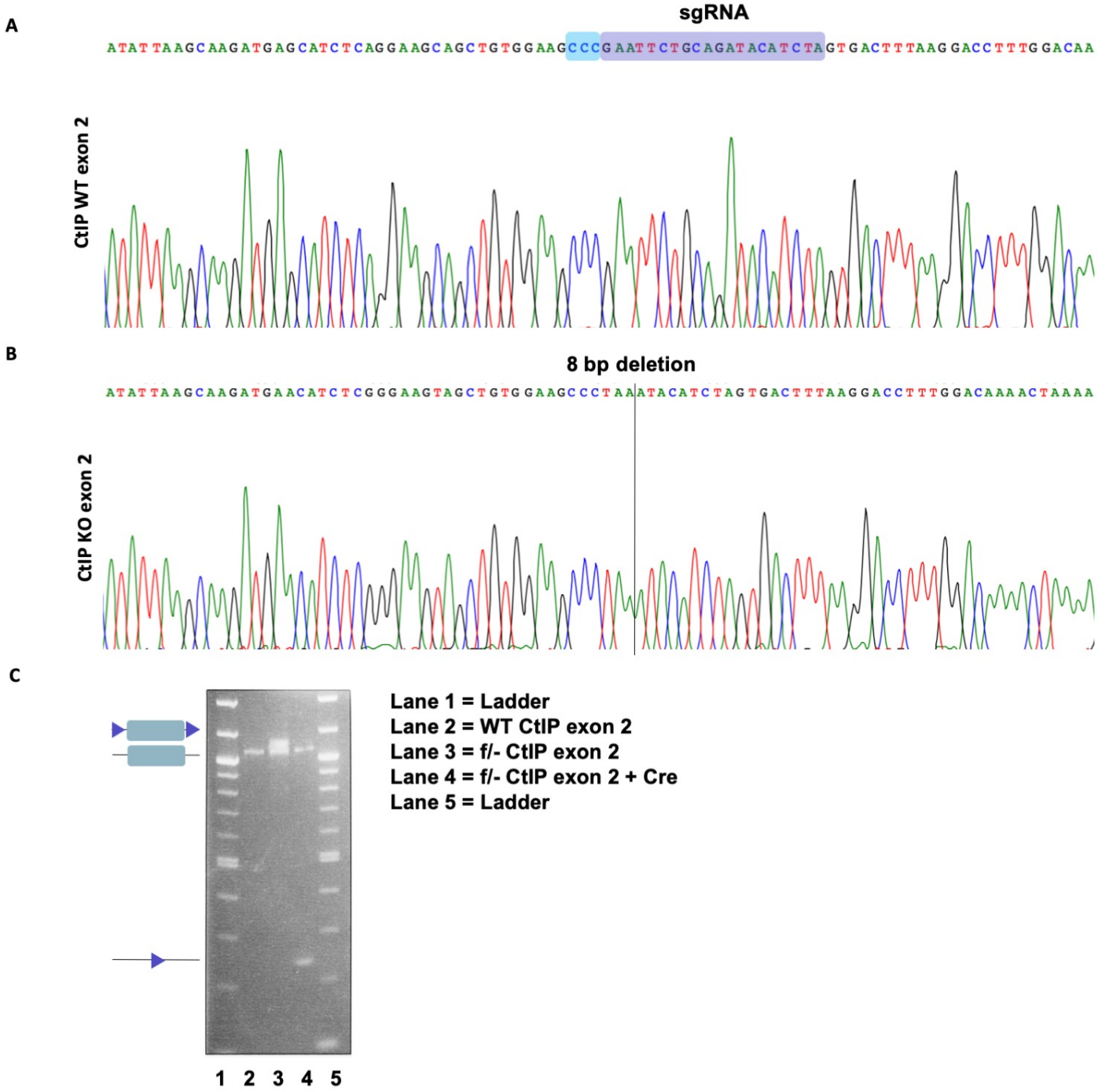

Figure S1. CtIP targeting strategy. (A) Partial sequence of the CtIP WT exon 2 with the sgRNA site highlighted in purple; the PAM site is highlighted in blue. (B) CRISPR-Cas9-induced 8 bp frameshift mutation in the non-floxed exon 2. (C) PCR confirmation of the floxed allele.

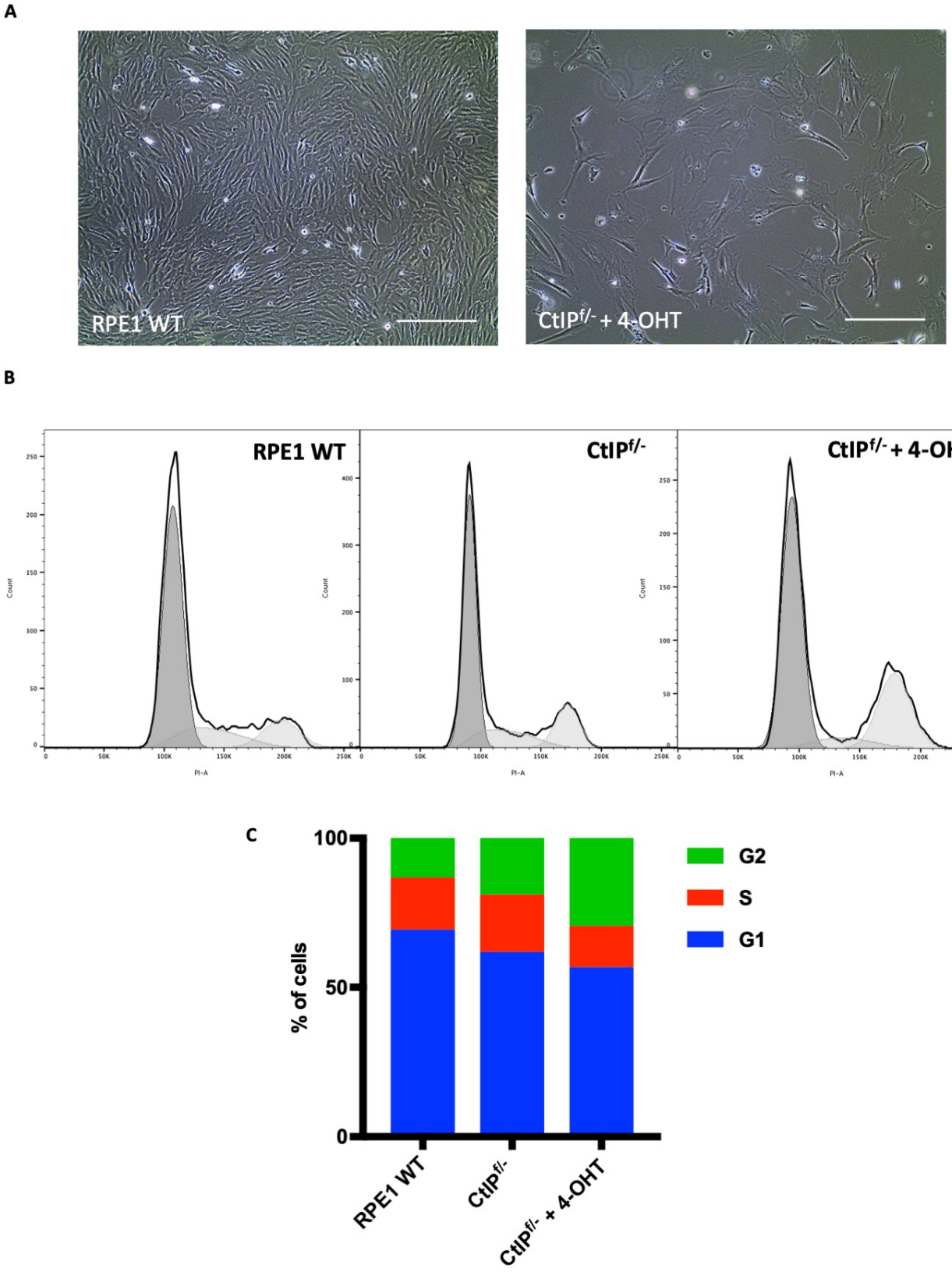

Figure S2. Loss of CtIP results in a G2 arrest. (A) Representative images of RPE1 WT cells and CtIP-null cells. (B) Cell cycle profiles of asynchronous cells stained with propidium iodide 2 days after 4-OHT or vehicle treatment. (C) Quantification of (B).

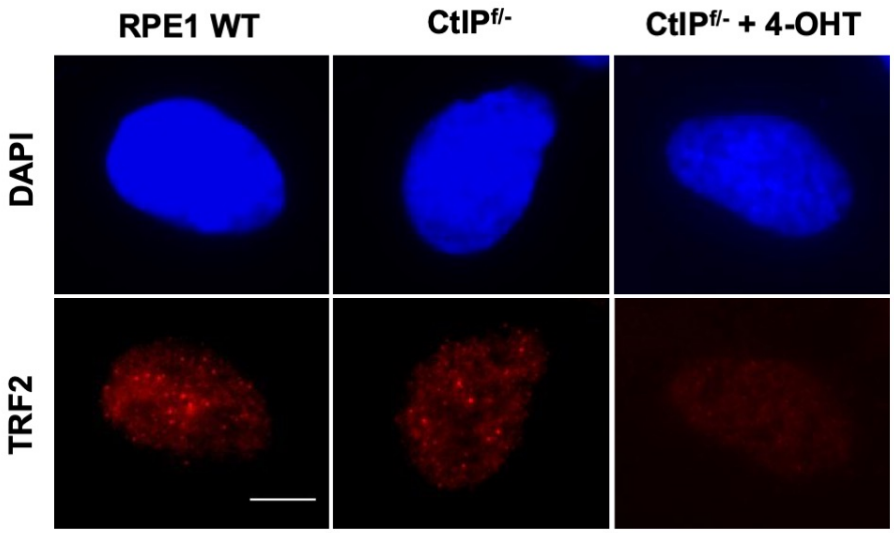

Figure S3. CtIP-deficient cells do not form TRF2 foci. IF staining of TRF2 in RPE1 WT, CtIP$^{f/-}$, CtIP$^{f/-}$ + 4-OHT.

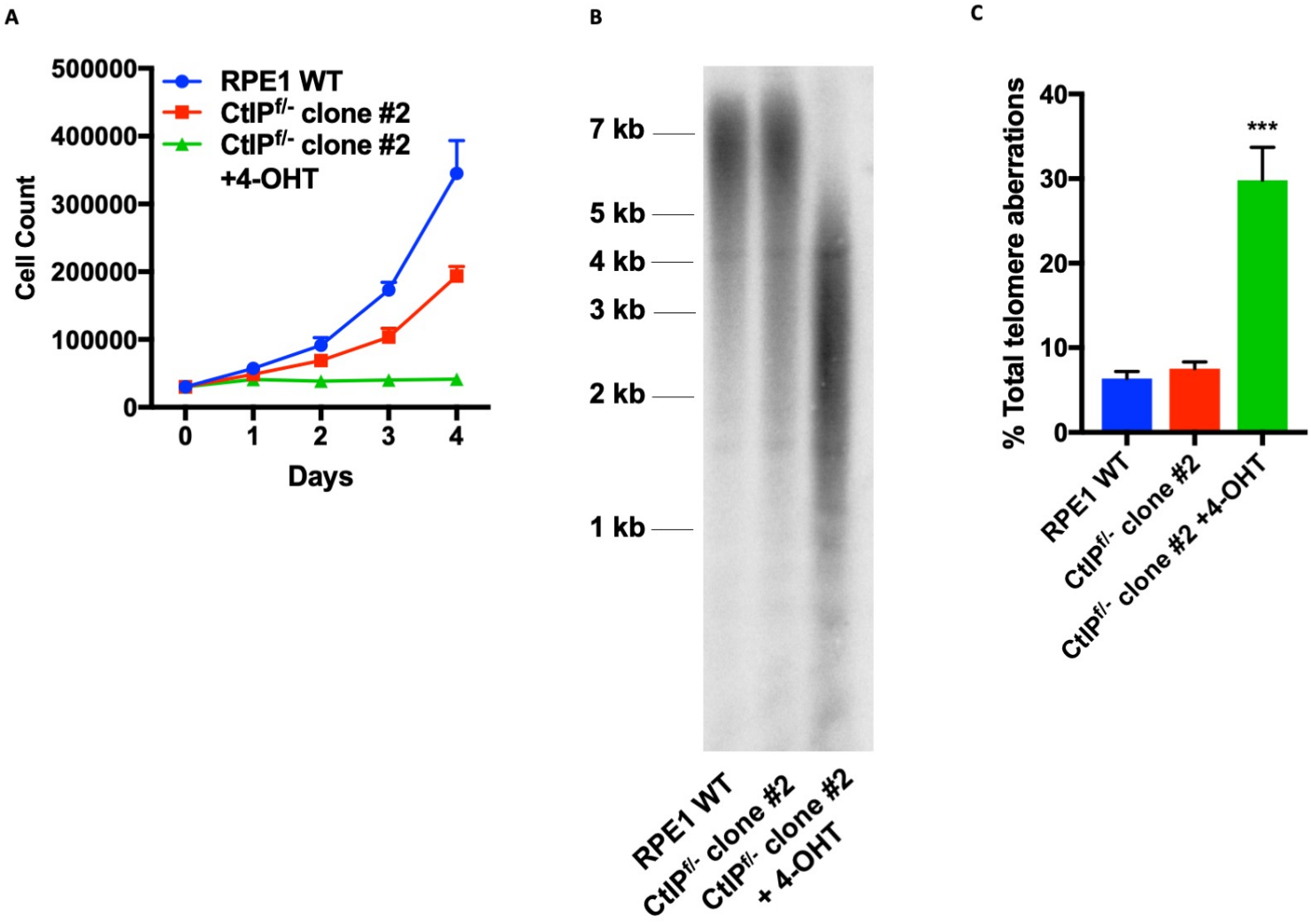

Figure S4. Characterization of an independently generated CtIP$^{f/-}$ clone. (A) Growth curve analysis of RPE1 WT, CtIP$^{f/-}$ #2, and CtIP$^{f/-}$ #2 +4-OHT. (B) TRF analysis of RPE1 WT, CtIP$^{f/-}$ #2, and CtIP$^{f/-}$ #2 +4-OHT after 2 days. (C) Quantification of total telomere aberrations by T-FISH analysis of RPE1 WT, CtIP$^{f/-}$ #2, and CtIP$^{f/-}$ #2 +4-OHT after 2 days. The aberrations scored include signal-free ends, fusions, breaks with telomeres, and internalized telomere signals; n = 2,000.

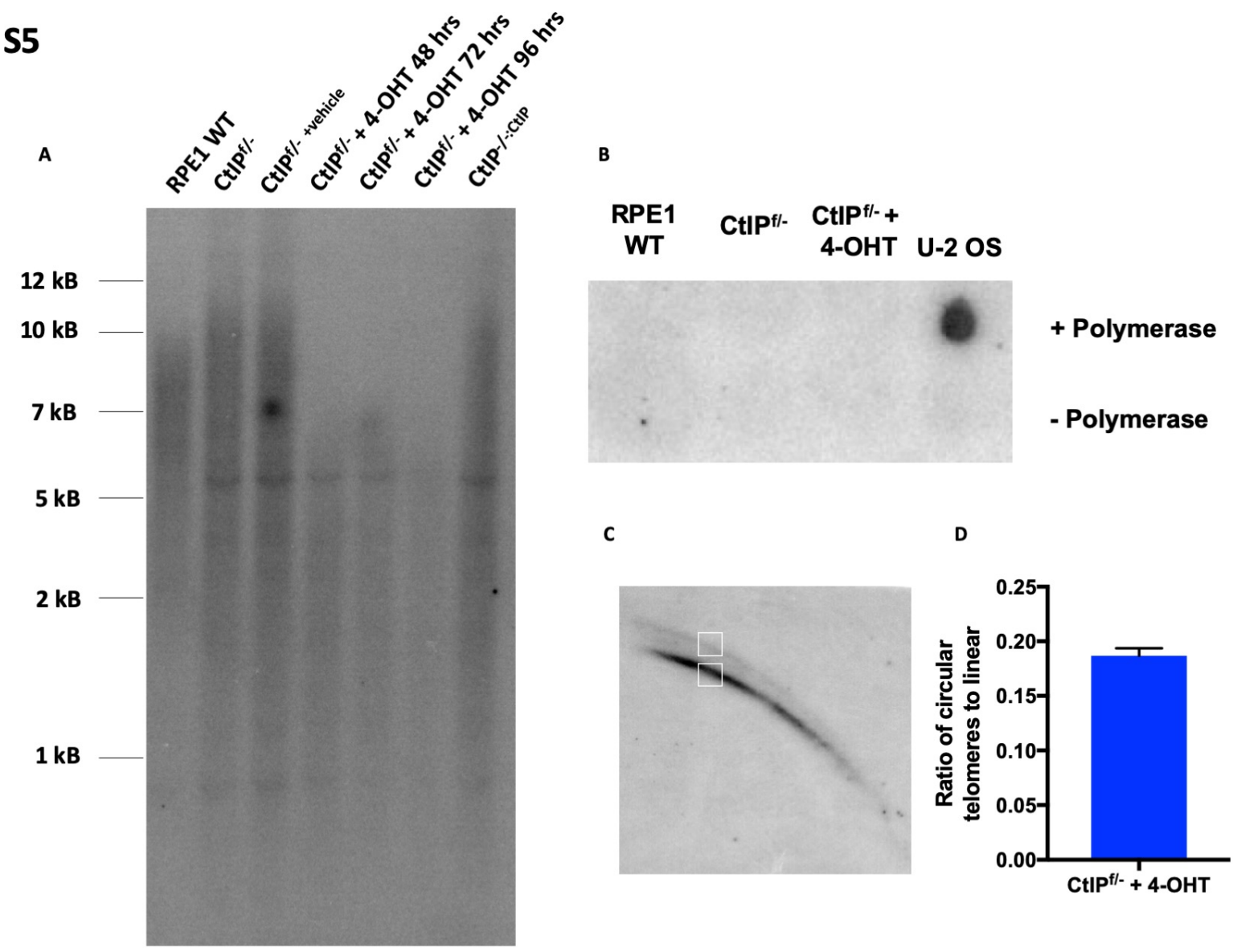

Figure S5. Telomere defects in the absence of CTIP. (A) TRF analysis of RPE1 WT, CtIP$^{f/-}$, CtIP$^{f/}$ + 4-OHT at varied time points, and CtIP$^{f/-:CtIP}$. (B) C-circle analysis of RPE1 WT, CtIP$^{f/-}$, CtIP$^{f/-}$ + 4-OHT, and U-2 OS cells. (C) Representative image of how densitometry was calculated on 2D telomere gels. (D) Quantification of densitometry analysis of circular telomeres to linear telomeres in CtIP$^{f/-}$ + 4-OHT.

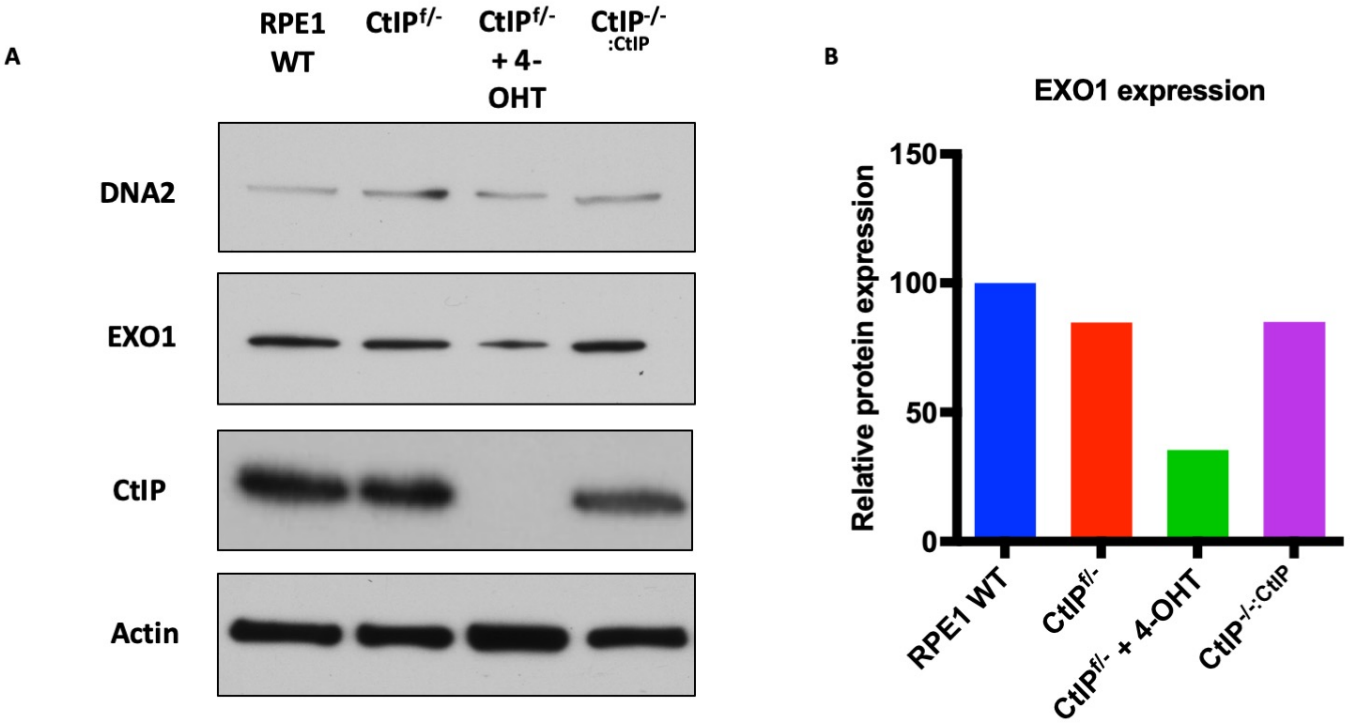

Figure S6. EXO1 expression decreases in the absence of CtIP. (A) Western blot analysis of DNA2, EXO1, and CtIP with actin as a loading control. (B). Quantification of EXO1 protein expression from (A).

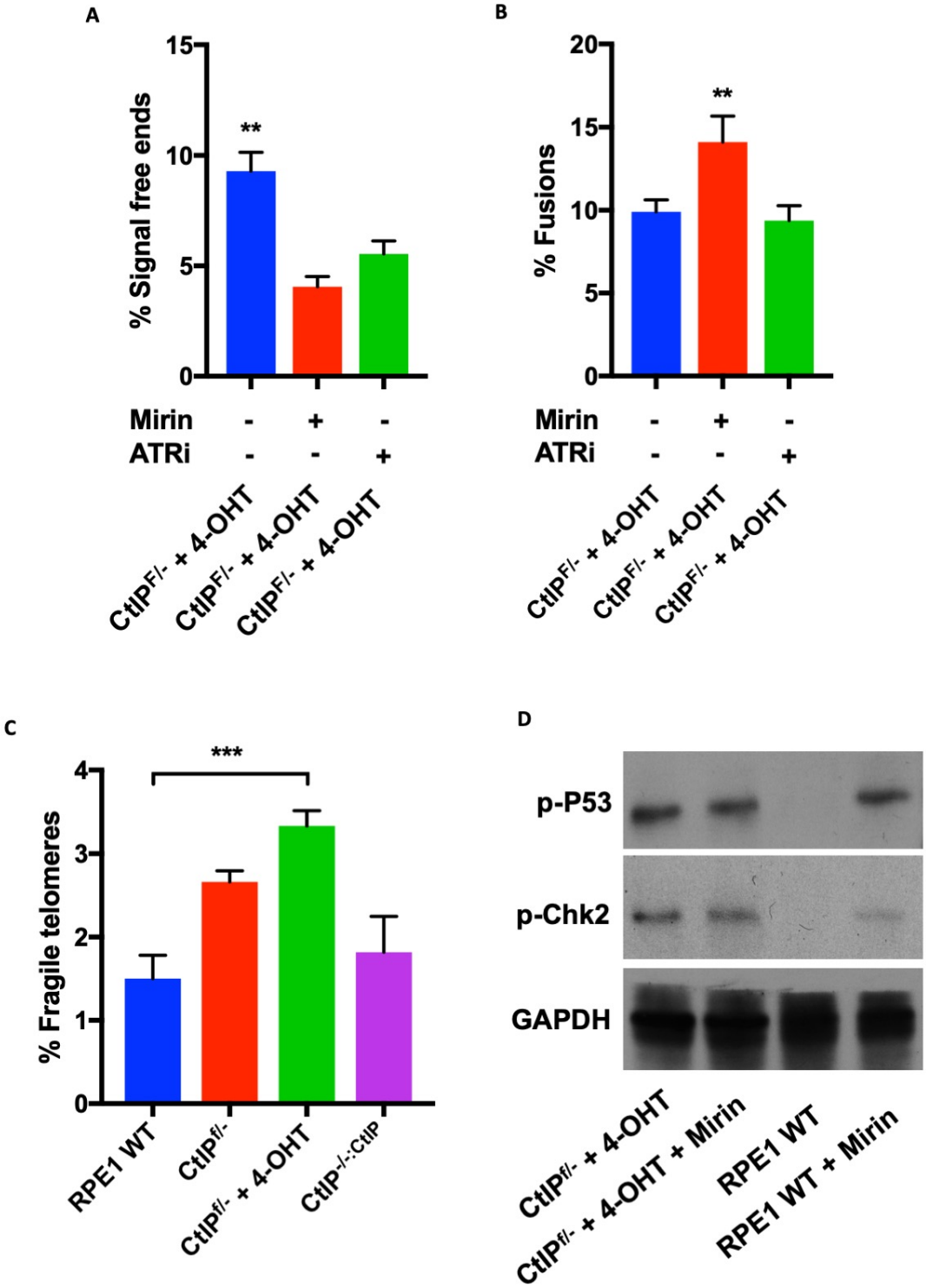

Figure S7. Individual telomere defects in the absence of CtIP. (A) Quantification of signal-free ends in CtIP$^{f/-}$ cells after treatment with 4-OHT for 36 hr and Mirin or ATRi for 24 hr. The data from 3 independent experiments is shown, n = 1,750; one way ANOVA and Tukey's test were used with $p < .01$ = **. (B) Quantification of all fusions in CtIP$^{f/-}$ cells after treatment with 4-OHT for 36 hr and Mirin or ATRi for 24 hr. The data from 3 independent experiments is shown, n = 1,750; one way ANOVA and Tukey's test were used with $p < .01$ = **. (C) Quantification of fragile telomeres in RPE1 WT, CtIP$^{f/-}$, CtIP$^{f/-}$ +4-OHT, and CtIP$^{-/-:CtIP}$. The data from 3 independent experiments is shown. n = 2,200; one way ANOVA and Tukey's test, $p < .001$ = ***. (D) Western blot analysis of phospho-Chk2 and phospho-p53 in RPE1 WT and CtIP$^{f/-}$ + 4-OHT with or without Mirin treatment for 24 hr.

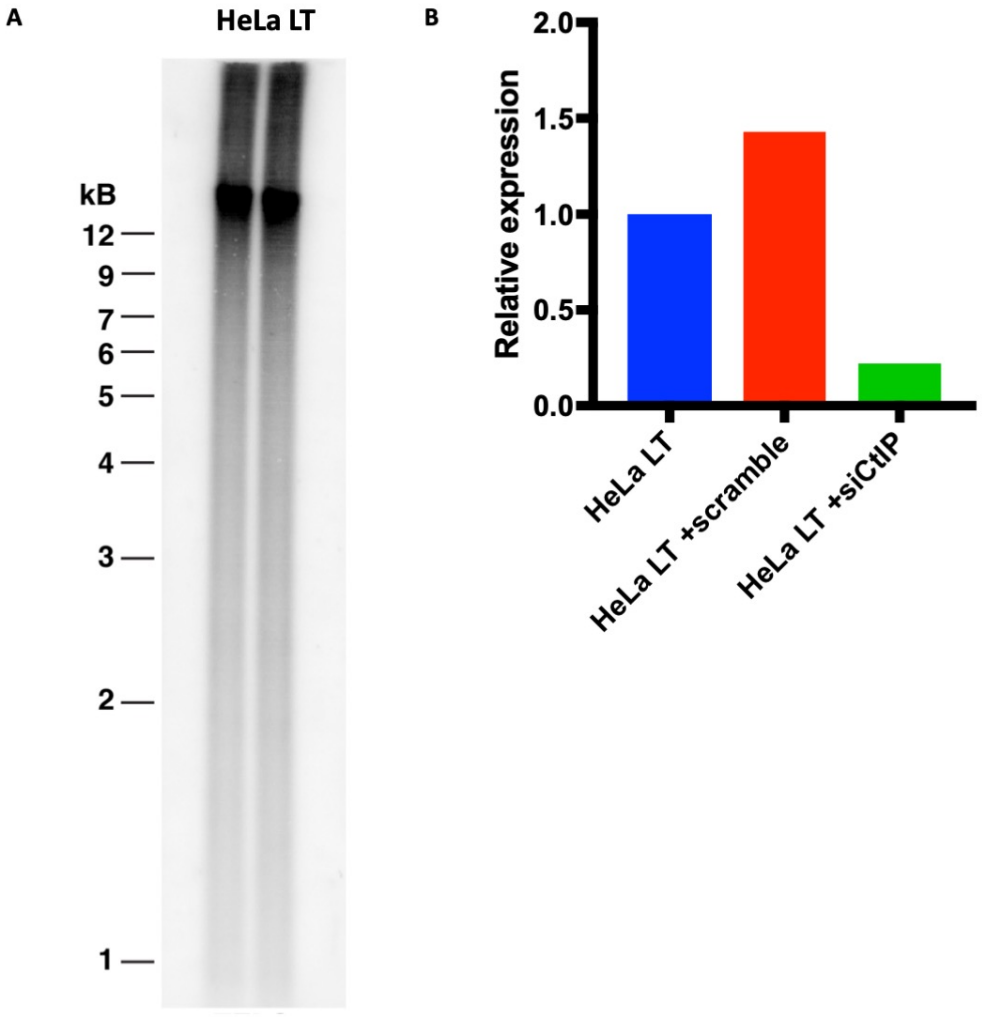

Figure S8. HeLa LT as a tool for telomere combing. (A) TRF of WT HeLa LT. (B) Quantification of CtIP knockdown in HeLa LT.

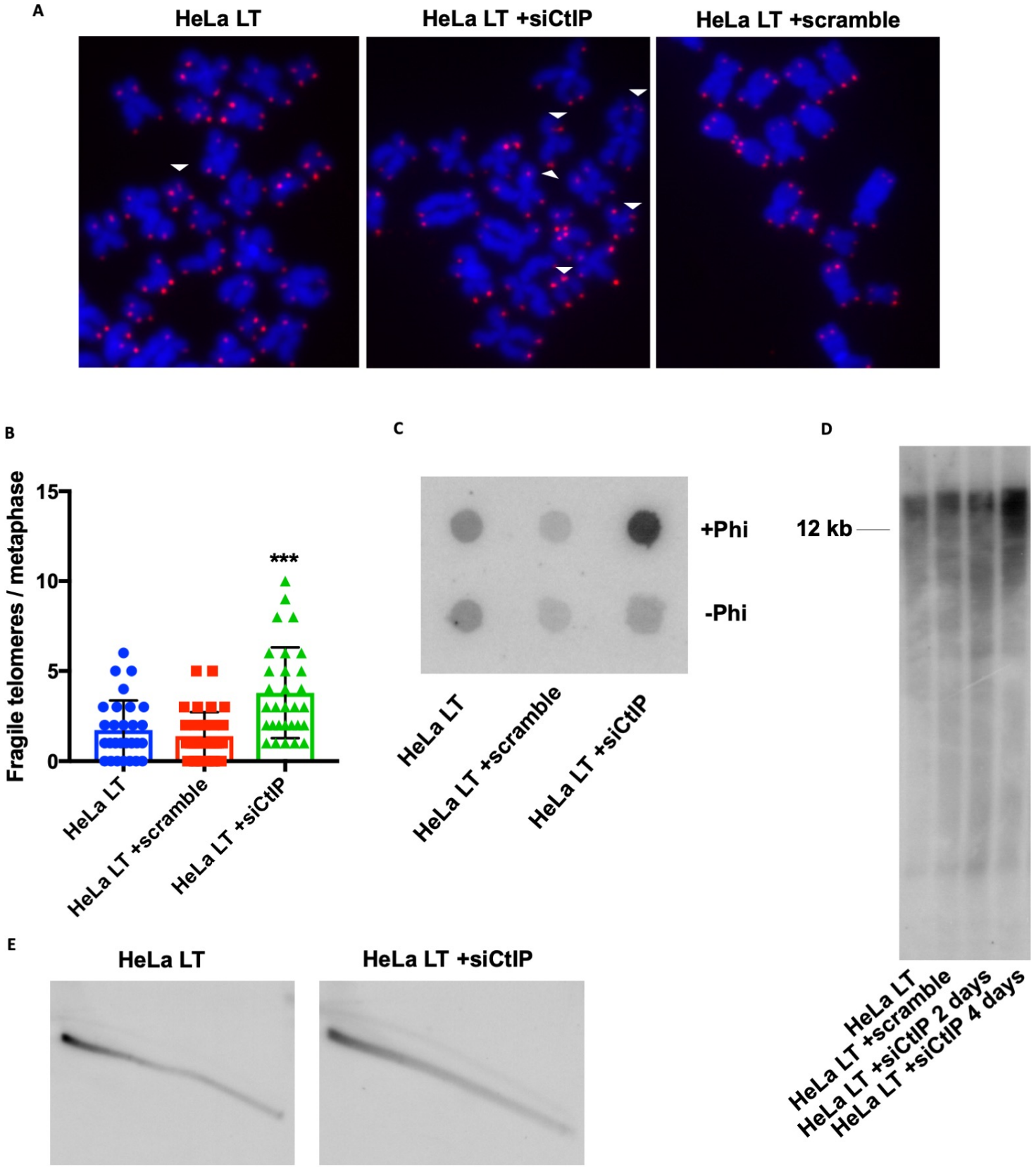

Figure S9. HeLa LT displays telomere abnormalities after CtIP depletion. (A) Representative images of fragile telomeres in HeLa LT, HeLa LT +scramble siRNA, and HeLa LT +siCTIP. (B). Quantification of fragile telomeres per metaphase from the T-FISH analysis (A). n = 30 metaphases. (C) C-circle quantification in HeLa LT, HeLa LT +scramble siRNA, and HeLa LT +siCTIP. (D) TRF analysis of HeLa LT, HeLa LT +scramble siRNA, and HeLa LT +siCTIP 2 days, and HeLa LT +siCTIP 4 days (double knockdown). (E) 2D gel analysis of telomeric DNA extracted from HeLa LT and HeLa LT +siCtIP for 2 days.